1000-0569/2011/027(12)-3640-52 *Acta Petrologica Sinica* 岩石学报

东天山黄山西含铜镍矿镁铁-超镁铁岩体岩浆地幔源区特征研究*

邓宇峰[1,2,3] 宋谢炎[1**] 陈列锰[1] 程松林[4] 张新利[5] 李军[5]

DENG YuFeng[1,2,3], SONG XieYan[1**], CHEN LieMeng[1], CHENG SongLin[4], ZHANG XinLi[5] and LI Jun[5]

1. 中国科学院地球化学研究所矿床地球化学国家重点实验室，贵阳 550002
2. 中国科学院研究生院，北京 100049
3. 合肥工业大学资源与环境工程学院，合肥 230009
4. 新疆地质矿产勘查开发局，乌鲁木齐 830000
5. 新疆地质矿产勘查开发局第六地质大队，哈密 839000

1. *State Key Laboratory of Ore Deposit Geochemistry, Institute of Geochemistry, Chinese Academy of Sciences, Guiyang* 550002, *China*
2. *Graduate University of Chinese Academy of Sciences, Beijing* 100049, *China*
3. *School of Resources and Environmental Engineering, Hefei University of Technology, Heifei* 230009, *China*
4. *Xinjiang Bureau of Geology and Exploration, Urumchi* 830000, *China*
5. *No. 6 Geological Team, Xinjiang Bureau of Geology and Exploration, Hami* 839000, *China*

2010-02-09 收稿，2010-04-20 改回.

Deng YF, Song XY, Chen LM, Cheng SL, Zhang XL and Li J. 2011. Features of the mantle source of the Huangshanxi Ni-Cu sulfide-bearing mafic-ultramafic intrusion, eastern Tianshan. *Acta Petrologica Sinica*, 27(12):3640 - 3652

Abstract Huangshan-Jingerquan copper-nickel mineralization belt is located in Late Paleozoic eastern Tianshan orogenic belt, which is part of the Central Asian orogenic belt. This mineralization belt is the second largest copper-nickel deposit base in China other than the Jinchuan deposit, with total reserves of copper, nickel up to one million tons. The Huangshanxi Cu-Ni ore deposit is one of the large deposits in the Huangshan-Jingerquan copper-nickel mineralization belt. The average grade of copper is 0.31%, with a total reserve of 188000 tons, average grade of nickel is 0.49%, with a total reserve of 32 million tons. The geochemical characteristics of the Huangshanxi rocks are significantly different from mafic-ultramafic rocks in Tarim large igneous province. The mafic-ultramafic intrusions in Huangshan-Jingerquan mineralization belt were emplaced at 269 ~ 298Ma, which were earlier than the mafic-ultramafic intrusions in Tarim large igneous province (272 ~ 274Ma). In addition, no Early Permian extensive flood basalt outcrop was observed. The Huangshanxi intrusuion is characterized by significant Nb, Ta, Ti negative anomalies, low $(^{87}Sr/^{86}Sr)_{269Ma}$ (0.7034 ~ 0.7037), and high $\varepsilon_{Nd(269Ma)}$ (5.14 ~ 7.14). These geochemical characteristics can not be explained by crustal contamination, but indicate that the primitive magma may be derived from partial melting of a metasomatized mantle source and formed in the active continental margin. However, the petrographic characteristics of the Huangshanxi intrusive rocks are different from Alaskan-type mafic-ultramafic intrusive rocks, therefore, it can not be excluded that partial melting of the metasomatized mantle occurred in a post-collisional extensional environment and the upwelling of asthenosphere may play an important role.

Key words Huangshan-Jingerquan Cu-Ni mineralization belt; Huangshanxi mafic-ultramafic intrusion; Magma Cu-Ni sulfide deposit; Metasomatized mantle; Asthenosphere

摘 要 新疆黄山-镜儿泉铜镍成矿带位于中亚造山带东天山晚古生代造山带，铜镍总储量达百万吨，是我国仅次于金川硫化物矿床的铜镍矿基地。黄山西铜镍矿床是该成矿带内一个大型矿床，Cu 平均品位是 0.31%，总储量 18.8×10^4 t，Ni 平均品

* 本文受国家自然科学重点基金项目(40730420、40973038)、中科院“百人计划”、中科院知识创新方向性项目(KZCX2-YW-Q04)和矿床地球化学国家重点实验室课题(KCZX20090105)联合资助.

第一作者简介：邓宇峰，男，1983 年生，博士，矿床地球化学专业，E-mail: dyfeng_214@sina.com

** 通讯作者：宋谢炎，男，1962 年生，研究员，岩石学与矿床地球化学专业，E-mail: songxieyan@vip.gyig.ac.cn

位是 0.49%，总储量 32×10^4t。黄山西岩体岩石地球化学特征与塔里木大火成岩省镁铁-超镁铁侵入岩和玄武岩存在明显差异; 较之塔里木大火成岩省镁铁-超镁铁岩体(269～274Ma)，黄山-镜儿泉铜镍成矿带镁铁-超镁铁岩体的形成更早(274～298Ma); 此外，成矿带内并没有早二叠溢流玄武岩大量出露。黄山西岩体各岩相的 MORB 标准化微量元素蛛网图显示明显的 Nb、Ta、Ti 负异常，$(^{87}Sr/^{86}Sr)_{269Ma}$ 值较低(0.7034～0.7037)，而 $\varepsilon_{Nd(269Ma)}$ 较高(5.14～7.14)，这些地球化学特征难以用地壳混染来解释，而显示其原始岩浆来自于交代地幔的部分熔融，表明原始岩浆可能形成于活动大陆边缘。然而，黄山西岩体的岩相学特征与阿拉斯加型岩体存在差别，因此，不能排除交代地幔的部分熔融发生于碰撞造山后的伸展阶段的可能，软流圈的上涌可能起到重要作用。

关键词 黄山-镜儿泉铜镍成矿带; 黄山西镁铁-超镁铁岩体; 岩浆铜镍矿床; 交代地幔; 软流圈
中图法分类号 P588.125

1 引言

中亚造山带位于西伯利亚与中朝-塔里木板块之间，从西到东横跨 5000km(图 1a)，它由大陆微地块、岛弧和大洋地壳混杂拼合构成(Sengör *et al.*，1993)。东天山造山带位于中亚造山带南部，夹于准噶尔地块与塔里木板块之间(图 1b)。不少学者认为东天山地区俯冲碰撞作用在中-晚石炭纪已经结束，从二叠世开始进入板内构造阶段(Zhou *et al.*，2004; 韩宝福等，2004; 王京彬和徐新，2006; 李锦轶等，

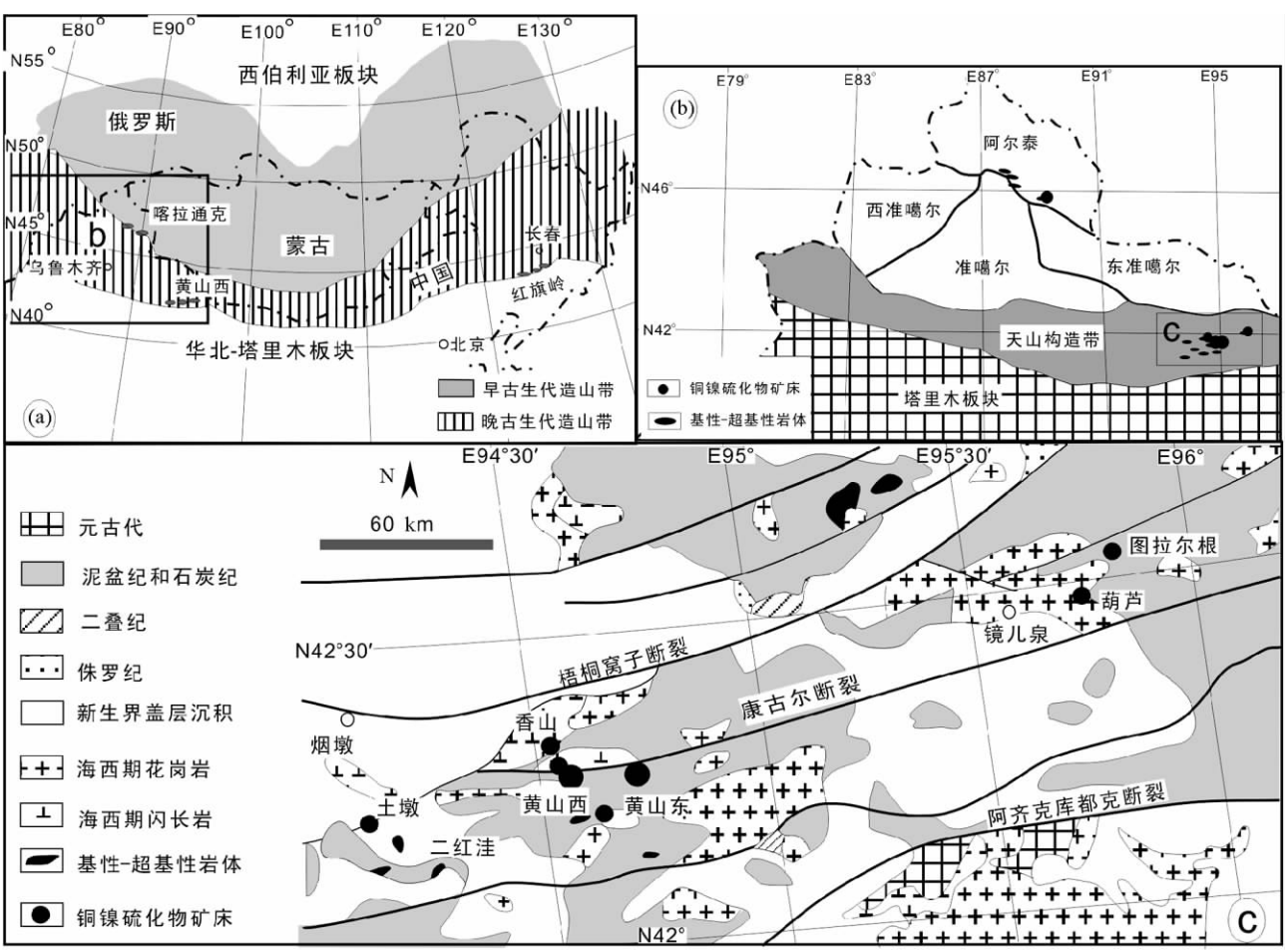

图 1 中亚造山带地质简图(a，据 Hong *et al.*，2004)、新疆北部构造纲要图(b，据新疆维吾尔自治区地质矿产局，1993)和黄山-镜儿泉铜镍硫化物成矿带地质简图(c，据王玉往等，2004)

Fig. 1 Schematic geological map of the Central Asian belt (a, after Hong *et al.*, 2004), tectonic domains of northern Xinjiang (b, after BGMRX, 1993) and simplified geological map of Huangshan-Jingerquan copper-nickel mineralization belt (c, after Wang *et al.*, 2004)

2006; Mao *et al.*, 2008)。黄山-镜儿泉铜镍成矿带位于东天山晚古生代造山带中段,东西长超过 270km,南北宽 10 ~ 15km(图 1c),现已查明黄山西(即黄山)和黄山东 2 个大型铜镍硫化物矿床以及香山、土墩、葫芦、图拉尔根 4 个中型铜镍硫化物矿床。这些矿床形成于晚古生代,铜镍总储量达百万吨,是我国仅次于甘肃金川的第二大岩浆硫化物矿床聚集区。

目前,关于黄山-镜儿泉铜镍成矿带含矿岩体形成的构造背景存在以下 4 种观点:(1)肖序常(1995)、马瑞士等(1997)和白云来(2000)认为该地区镁铁-超镁铁岩体是蛇绿岩套;(2)胡受奚等(1990)、刘德权(1983)和 Xiao *et al.* (2008)认为这些岩体形成于活动大陆边缘;(3)秦克章(2000)、韩宝福等(2004)、王京彬和徐新(2006)、李锦轶等(2006)、顾连兴等(2006)、Mao *et al.* (2008)和夏明哲(2009)认为岩体形成于造山后岩石圈伸展环境;(4)Zhou *et al.* (2004)、毛景文等(2006)和 Pirajno *et al.* (2008)则认为含矿岩体的形成与地幔柱有关。由于活动大陆边缘和造山后伸展环境的镁铁质岩浆都起源于交代地幔的部分熔融,与地幔柱岩浆以及蛇绿岩套的地球化学特征有显著差异,因此,通过对岩体地球化学特征的研究明确其地幔源区特征是探讨成矿构造背景的关键。黄山西岩体是黄山-镜儿泉铜镍成矿带上规模较大、含矿性最好的典型岩体,虽然 Zhou *et al.* (2004)和夏明哲(2009)认为黄山西岩体源区岩浆源于软流圈和俯冲流体交代地幔的部分熔融,但是夏明哲(2009)没有深入探讨该岩体与地幔柱的成因关系,而 Zhou *et al.* (2004)认为该岩体是地幔柱活动产物,本文试图通过研究黄山西岩体的岩石地球化学特征,并与塔里木大火成岩省进行对比,探讨其地幔源区特征,为进一步论证黄山-镜儿泉铜镍成矿带形成的构造背景提供佐证。

2 岩体地质背景

东天山晚古生代造山带夹于吐哈地块与中天山地块之间,依据古生代地层系统及重要断裂的分布,东天山可分为北、中、南 3 条地层-构造带(王京彬等, 2006)。北带位于康古尔断裂以北的吐哈盆地南缘,主要出露从奥陶系到石炭系岛弧火山岩及海相凝灰岩和砂岩;中带为康古尔剪切带,夹于康古尔断裂和雅满苏断裂之间,主要为复理石建造(下石炭统干墩组)和拉斑玄武岩-硅质岩-泥质岩等深水相组合(中石炭统梧桐窝子组);南带位于雅满苏大断裂与阿奇克库都克大断裂之间,该区缺乏奥陶-泥盆系,下石炭统以玄武岩和中酸性火山碎屑岩、熔岩为主,阿奇克库都克断裂以南为具有前寒武基底的中天山地块。黄山-镜儿泉铜镍成矿带含矿岩体沿康古尔剪切带展布,侵入于泥盆-石炭系地层中,本文研究的黄山西镁铁-超镁铁岩体位于康古尔剪切带西段(图 1c)(王玉往等, 2004)。

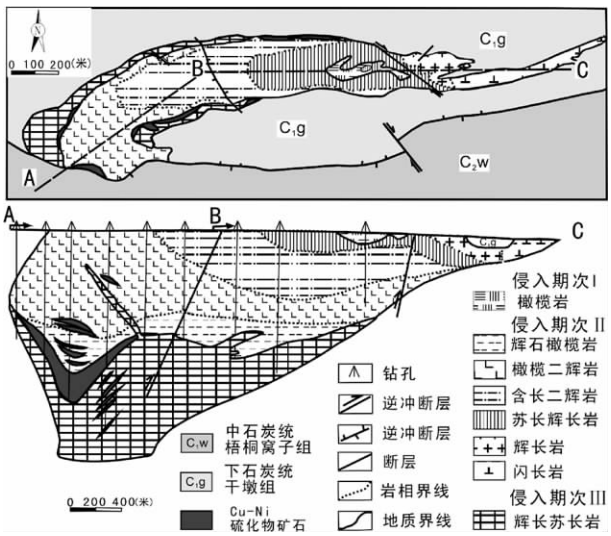

图 2 黄山西岩体地质平面图及剖面图(据李德惠等, 1989)

Fig. 2 Simplified geological map and a cross section of the Huangshanxi intrusion, showing the distribution of lithological units and sulfide ore bodies

3 岩体岩相学特征

黄山西岩体长约 3.8km,平均宽约 0.45km,平面上呈西宽东窄的不规则的蝌蚪状,出露面积 1.71km^2(图 2)。岩体侵位于下石炭统干墩组灰岩、变余砂岩和细碧玢岩中。岩体主体从西向东依次出露辉长苏长岩、辉石橄榄岩、橄榄二辉岩、含长二辉岩、苏长辉长岩、橄榄岩、辉长岩和闪长岩;剖面上从下向上依次为辉长苏长岩、辉石橄榄岩、橄榄二辉岩、含长二辉岩、苏长辉长岩、辉长岩和闪长岩(图 2)。辉石橄榄岩、橄榄二辉岩、含长二辉岩、苏长辉长岩、辉长岩和闪长岩构成岩体的主体,各岩相之间呈渐变过渡关系。橄榄岩出现于岩体中东部,为一无根上悬体,与苏长辉长岩呈侵入接触关系,局部见苏长辉长岩呈岩脉贯入橄榄岩中(李德惠等, 1989①)。西部边缘辉长苏长岩与主岩体辉石橄榄岩呈侵入接触关系,辉长苏长岩明显地穿插在辉石橄榄岩和橄榄二辉岩中。

上述岩相特征表明黄山西岩体是多次岩浆侵位的结果:岩体中部橄榄岩上悬体是第一次岩浆侵入的残留体;岩体的主体是第二次侵入的岩浆的堆积相;而岩体边缘的辉长苏长岩是第三次岩浆从岩体底部和边缘侵入的结果(李德惠等, 1989)。

岩浆铜镍硫化物矿体赋存于黄山西岩体主体的下部和

① 李德惠,包相臣,张伯南等. 1989. 黄山铜镍成矿带地质、地球物理和地球化学综合研究及找矿靶区优选报告. 新疆 305 项目组报告(内部资料)

底部,包括 30 号和 31 号规模较大的矿体和若干规模较小的矿体,其中 P30 矿体金属储量约占整个矿床储量的 85% 以上,矿石平均品位: Cu 0.31%,Ni 0.48%,Co 0.03%。各个矿体中低品位的贫矿石占主导地位,Ni > 1% 的富矿所占比例很小(李德惠等, 1989)。矿石矿物主要有磁黄铁矿、镍黄铁矿、黄铜矿、紫硫镍矿、马基诺矿、黄铁矿、方黄铜矿等。

4 样品分析方法

常量和微量元素在中国科学院矿床地球化学国家重点实验室测定。常量元素的测定采用 x 射线荧光光谱法(XRF),其过程大致如下: 首先称取 0.7g 样品,然后加入适量硼酸高温熔融成玻璃片,最后采用外标法测定氧化物含量,分析误差为 1% ~3%。微量元素测定采用等离子质谱(ICP-MS)法: 首先称取 50mg 样品,用酸溶样制成溶液,然后在 ICP-MS 上用内标法进行测定。微量元素具体分析方法见 Qi *et al.* (2000)。

Rb-Sr、Sm-Nd 同位素分析在中国地质大学(武汉)地质过程与矿产资源国家重点实验室测定。分析方法如下: 称取 0.1 ~1g 处理好的粉末样品,置于聚四氟乙烯封闭容器中,加入适量的混合稀释剂,用 HF 和 $HClO_4$ 在微波炉中分解样品并使其完全转化成过氯酸盐,采用阳离子交换法分离 Rb 和 Sr。Rb-Sr 同位素分析在 POEMS Ⅲ 上进行,用标准样品 NBS987 和 La Jolla 监控分析流程,NBS987 = 0.710255 ±4,La Jolla = 0.511846 ±1。Pb 同位素在核工业北京地质研究院分析测试研究中心测定。其具体分析方法同张桂存等(1999)。

5 分析结果

5.1 主量元素

文中黄山西样品采自岩体第二期(含长二辉岩、橄榄二辉岩和辉石橄榄岩)和第三期侵入岩石(辉长苏长岩)。从样品常量元素和微量元素测试分析结果(表 1)可以看出,样品具有较宽的成分变化,如 MgO 含量为 6.97% ~38.1%。辉石橄榄岩、橄榄二辉岩和含长二辉岩中 $Fe_2O_3^T$ 与 MgO 之间的正相关关系(图 3c),以及 CaO、Al_2O_3 与 MgO 呈负相关(图 3b, d),这些特征表明它们是橄榄石、斜方辉石和单斜辉石为主的堆积相,而辉长苏长岩和辉长岩中 CaO 与 MgO 的正相关关系(图 3d),以及 $Fe_2O_3^T$、Al_2O_3 与 MgO 呈负相关关系(图 3b, c)指示单斜辉石和斜长石的堆积。矿物的分离结晶导致了岩相间常量元素的有规律性变化,不同期次岩石之间氧化物组成的规律性变化表明它们为同源岩浆分异的产物。

5.2 微量元素

岩体微量元素分析结果见表 1,在 MORB 标准化微量元

表 1 黄山西岩体常量元素(wt%)、微量元素($\times 10^{-6}$)分析测试结果

Table 1 Contents of oxides (wt%) and trace ($\times 10^{-6}$) elements of the Huangshanxi intrusive rock

岩性	辉长苏长岩			含长二辉岩			橄榄二辉岩	
样品号	XH05-36	XH08-1	XH05-30	XH08-5	XH08-6	XH08-7	XH05-11	XH05-28
SiO_2	52.8	52.8	52.3	49.7	47.6	50.2	47.1	46.9
TiO_2	0.66	1.12	0.59	0.42	0.38	0.43	0.31	0.29
Al_2O_3	18.0	17.9	17.7	4.80	5.04	5.06	3.85	4.72
$Fe_2O_3^T$	7.24	7.97	6.78	8.45	9.20	7.62	10.6	11.0
MnO	0.12	0.14	0.11	0.17	0.17	0.16	0.17	0.13
MgO	6.90	6.23	6.92	19.8	21.7	17.7	27.1	27.6
CaO	9.38	8.86	8.95	14.7	11.4	15.7	7.34	5.99
Na_2O	3.36	2.95	3.38	0.36	0.40	0.49	0.47	0.80
K_2O	0.45	0.51	0.27	0.08	0.08	0.19	0.17	0.22
P_2O_5	0.08	0.17	0.07	0.06	0.06	0.08	0.04	0.05
LOI	0.32	1.88	1.72	1.23	3.47	1.55	1.44	1.14
Total	99.3	100.6	98.8	99.8	99.6	99.1	99.0	98.8
Sc	24.4	26.1	28.6	58.3	48.5	66.7	23.3	31.3
V	145	183	140	250	192	311	76.2	91.5
Cr	162	138	163	2000	1980	989	1813	2119
Co	44.4	27.5	38.9	70.8	76.6	54.8	77.5	104
Ni	31.9	21.1	38.6	195	181	121	312	440
Cu	34.0	14.3	17.4	66.1	63.8	46.0	50.8	56.0
La	4.14	8.61	4.21	1.20	1.60	1.65	2.09	2.41
Ce	9.44	19.8	9.58	3.89	4.25	4.84	4.47	5.41
Pr	1.36	2.82	1.45	0.73	0.70	0.87	0.68	0.77
Nd	6.39	12.5	6.66	4.07	3.55	4.84	3.36	3.79
Sm	1.62	3.34	1.48	1.51	1.28	1.78	0.88	0.97
Eu	0.79	1.19	0.67	0.48	0.39	0.55	0.23	0.28
Gd	1.97	3.29	1.54	1.68	1.34	2.06	1.02	0.91
Tb	0.33	0.62	0.31	0.33	0.28	0.39	0.18	0.20
Dy	1.92	3.65	1.86	2.13	1.75	2.62	1.03	1.15
Ho	0.40	0.82	0.39	0.48	0.39	0.56	0.21	0.24
Er	1.14	2.15	1.16	1.20	1.05	1.49	0.58	0.62
Tm	0.15	0.30	0.15	0.17	0.15	0.20	0.09	0.10
Yb	1.10	2.03	0.95	1.09	0.91	1.31	0.56	0.58
Lu	0.15	0.29	0.14	0.15	0.14	0.19	0.09	0.10
Rb	6.16	13.0	5.24	1.59	1.17	6.09	4.43	5.08
Sr	418	405	394	54.3	64.0	78.3	82.3	88.8
Ba	116	165	100	14.9	20.2	39.5	46.7	49.8
Y	12.0	20.3	12.7	11.0	9.4	13.4	6.37	7.25
Nb	1.27	3.23	1.22	0.29	0.44	0.41	0.46	0.58
Ta	0.09	0.25	0.12	0.04	0.04	0.04	0.04	0.07
Zr	37.4	104	37.1	27.1	28.4	32.4	21.9	28.2
Hf	1.03	2.83	1.21	0.95	0.89	1.12	0.65	0.82
Th	0.57	1.63	0.65	0.13	0.29	0.25	0.56	0.60
U	0.24	0.62	0.24	0.06	0.13	0.11	0.19	0.22
Pb	2.80	4.40	2.85	0.47	0.65	1.04	1.66	2.48

续表 1

Continued Table 1

岩性	橄榄二辉岩		辉石橄榄岩				
样品号	XH08-4	XH05-32	XH05-4	XH05-9	XH05-25	XH05-27	XH05-33
SiO_2	48.0	46.5	39.5	45.5	40.6	42.2	46.1
TiO_2	0.36	0.28	0.22	0.26	0.19	0.26	0.28
Al_2O_3	5.74	4.09	3.61	3.53	2.93	4.20	4.07
$Fe_2O_3^T$	9.69	11.2	11.5	11.6	11.0	11.6	11.5
MnO	0.16	0.17	0.16	0.18	0.15	0.11	0.17
MgO	22.0	27.6	35.1	29.8	30.8	31.1	29.3
CaO	11.7	6.75	1.57	5.51	1.81	2.44	5.75
Na_2O	0.41	0.57	0.27	0.34	0.09	0.49	0.56
K_2O	0.11	0.21	0.27	0.13	0.08	0.26	0.22
P_2O_5	0.07	0.04	0.05	0.03	0.04	0.05	0.05
LOI	1.59	1.81	6.45	1.45	10.6	6.04	1.39
Total	99.8	99.6	99.0	98.6	98.6	98.7	99.7
Sc	47.7	25.1	11.3	23.5	13.9	18.7	22.6
V	189	83.2	43.2	68.9	35.2	59.8	76.0
Cr	2200	1992	1959	1899	1971	2082	1819
Co	87.6	95.3	106	77.6	91.4	116	86.6
Ni	334	502	863	363	700	904	412
Cu	73.0	91.8	232	50.3	82.3	189	64.8
La	1.37	2.51	2.18	2.21	2.02	2.51	2.39
Ce	3.78	5.78	4.93	4.95	4.80	5.13	5.23
Pr	0.69	0.89	0.75	0.70	0.74	0.68	0.75
Nd	3.52	4.26	3.19	3.10	3.42	3.24	3.69
Sm	1.26	1.00	0.75	0.84	0.81	0.84	0.83
Eu	0.45	0.33	0.22	0.26	0.47	0.24	0.27
Gd	1.33	1.26	0.90	1.03	0.82	0.83	1.05
Tb	0.29	0.22	0.15	0.15	0.17	0.15	0.19
Dy	1.72	1.28	0.83	1.01	0.97	0.89	1.12
Ho	0.38	0.27	0.17	0.20	0.19	0.17	0.24
Er	1.00	0.79	0.46	0.62	0.59	0.51	0.63
Tm	0.15	0.11	0.08	0.09	0.08	0.08	0.09
Yb	0.89	0.66	0.46	0.53	0.46	0.45	0.57
Lu	0.14	0.09	0.07	0.08	0.07	0.09	0.09
Rb	3.19	4.89	6.40	4.65	2.75	5.69	5.26
Sr	105	89.4	67.4	68.9	27.3	70.9	87.1
Ba	35.3	53.4	64.5	49.6	20.5	66.0	56.6
Y	9.54	7.57	4.81	5.83	5.78	5.24	6.35
Nb	0.29	0.63	0.74	0.46	0.61	0.73	0.56
Ta	0.04	0.06	0.06	0.04	0.05	0.08	0.06
Zr	29.5	26.5	24.3	20.5	14.4	24.1	25.2
Hf	0.89	0.81	0.71	0.64	0.46	0.86	0.72
Th	0.24	0.54	0.51	0.48	0.47	0.60	0.56
U	0.10	0.20	0.20	0.17	0.17	0.20	0.23
Pb	0.70	1.75	5.62	1.85	3.68	2.43	1.72

素蛛网图中(图 4),黄山西样品总体上表现为大离子亲石元素(Rb、Ba、Sr)相对富集,而部分高场强元素(Nb、Ta、Ti)相对亏损。而被认为是地幔柱活动产物的塔里木地区瓦吉里塔格地区镁铁-超镁铁岩和巴楚地区辉绿岩墙(姜常义等,2004a; Zhou *et al.*, 2009)、以及峨眉山大火成岩省力马河岩体(陶琰等,2007)不仅所有微量元素含量都明显高于黄山西岩体,而且 Nb、Ta 和 Ti 的亏损程度也远远弱于黄山西岩体。然而,黄山西岩体微量元素蛛网图与阿拉斯加型 Quetico 岩体(Pettigrew and Hattori, 2006)相似,两者都具有大离子亲石元素的富集和相似的 Nb、Ta、Ti 亏损(图 4)。

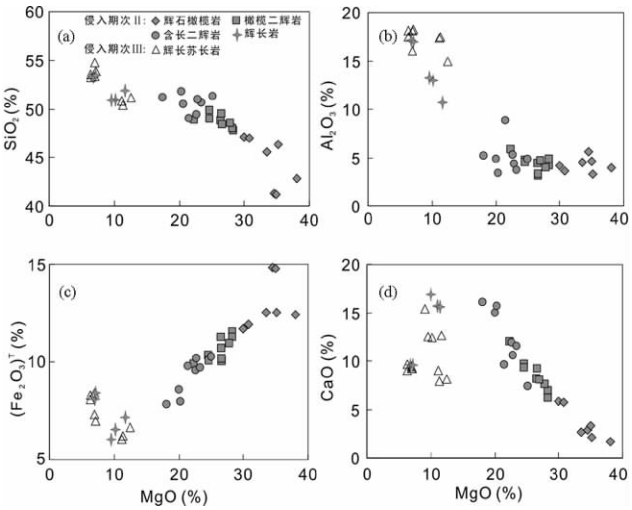

图 3 黄山西岩体哈克图解

部分数据来自 Zhou *et al.* (2004) **和夏明哲**(2009)

Fig. 3 Haker diagrams of the Huangshanxi intrusive rocks

Some data are cited from Zhou *et al.* (2004) and Xia (2009)

5.3 同位素

黄山西岩体具有低的、变化较小的 $(^{87}Sr/^{86}Sr)_{269Ma}$ (0.7034~0.7037),而 $\varepsilon_{Nd(269Ma)}$ 较高,变化范围也较小,介于 5.14~7.14 之间(表 2)。在 $\varepsilon_{Nd(269Ma)}$-$(^{87}Sr/^{86}Sr)_{269Ma}$ 图解(图 5)中,黄山西岩体的样品与阿拉斯加型岩体相似投影范围投点在岛弧、活动大陆边缘和洋岛玄武岩(OIB)的重叠区域,但 $\varepsilon_{Nd(269Ma)}$ 明显高于塔里木大火成岩省瓦吉里塔格地区超镁铁岩、巴楚岩体、麻扎尔塔格地区岩墙和柯坪玄武岩(姜常义等, 2004a, b, c; Zhang *et al.*, 2008; Zhou *et al.*, 2009)。Pb 同位素比值低,变化也较小,$^{206}Pb/^{204}Pb$ 比值为 18.04~18.19,$^{207}Pb/^{204}Pb$ 比值为 15.46~15.48,$^{207}Pb/^{204}Pb$ 比值为 37.59~37.66(表 2)。

6 讨论

如前所述,黄山-镜儿泉成矿带内镁铁-超镁铁岩体形成的构造背景存在较大争论,近年来越来越多的证据已经证明黄山-镜儿泉成矿带内镁铁-超镁铁岩体不是蛇绿岩套的侵入岩体(朱文斌等, 1996; 毛景文等, 2002),所以,争论的焦点在于镁铁-超镁铁岩体是否与二叠纪塔里木地幔柱有关。本文认为岩体形成时间是否与塔里木地幔柱相吻合及地幔源区性质是确定黄山-镜儿泉成矿带构造背景的关键。

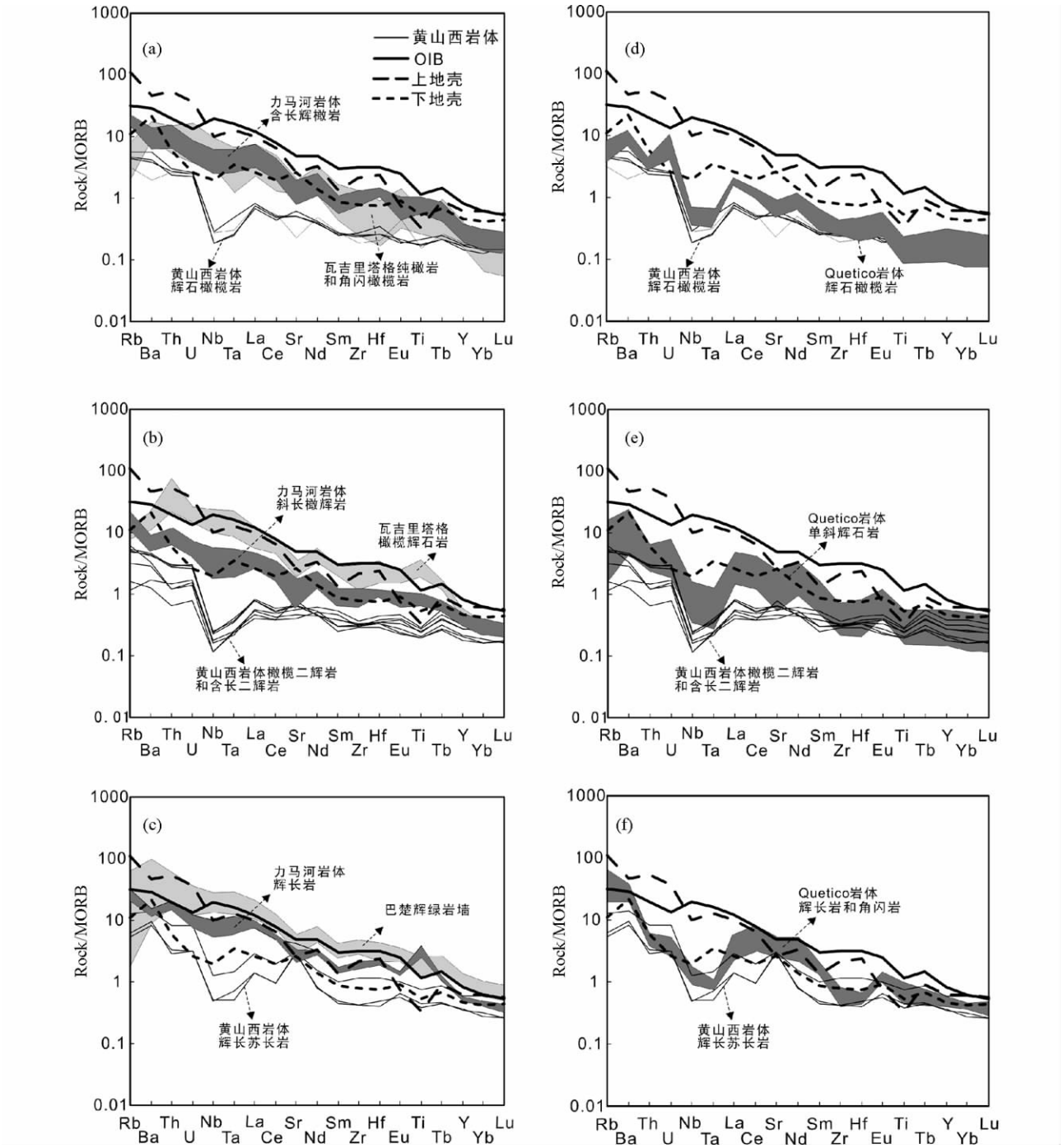

图 4 黄山西岩体 MORB 标准化微量元素蛛网图

(a)、(b)、(c) **分别显示黄山西岩体橄榄岩、辉石岩、辉长岩与力马河岩体橄榄岩、辉石岩、辉长岩(** 陶琰等, 2007) **,塔里木大火成岩省瓦吉里塔格橄榄岩(** 姜常义等, 2004a) **和辉石岩(** 姜常义等, 2004b) **、巴楚辉绿岩墙(** Zhou *et al.* , 2009) **和洋岛玄武岩(** Sun and McDonough, 1989) **的微量元素配分模式的差异;(**d) 、(e) 、(f) **显示黄山西岩体橄榄岩、辉石岩、辉长岩与阿拉斯加型** Quetico **岩体橄榄岩、辉石岩、辉长岩(** Pettigrew and Hattori, 2006) **微量元素配分模式相似; 上地壳与下地壳数据来自** Rudnick and Fountain (1995)

Fig. 4 N-MORB normalized spidergrams for the Huangshanxi intrusive rocks

(a), (b), (c) – show that the Huangshanxi peridotites, pyroxenites, gabbros have trace element compositions different from the peridotites, pyroxenites, gabbros of the Limahe intrusion, the peridotites (Jiang *et al.* , 2004a) and pyroxenites (Jiang *et al.* , 2004b) of Wajilitag, mafic dykes of Babu in Tarim large igneous province (Zhou *et al.* , 2009) and OIB (Sun and McDonough, 1989); (d), (e), (f) – show that the trace element contents of the Huangshanxi peridotites, pyroxenites, gabbros are similar to those of the Quetico intrusion rocks (Pettigrew and Hattori, 2006), the data of upper crust and lower crust are from Rudnick and Fountain (1995)

表 2 黄山西岩体 Sr、Nd、Pb 同位素分析数据

Table 2 Sr, Nd, Pb isotope data of the Huangshanxi intrusion

岩性	辉石橄榄岩			橄榄二辉岩			辉长苏长岩
样品号	XH05-4	XH05-9	XH05-33	XH05-11	XH05-28	XH05-32	XH05-36
Rb($\times10^{-6}$)	6.4	4.65	5.26	4.43	5.08	4.89	6.16
Sr($\times10^{-6}$)	67	69	87	82	89	89	418
$^{87}Sr/^{86}Sr$	0.704616	0.704126	0.704341	0.704266	0.704284	0.704243	0.703753
$2\sigma_m$	3	5	4	5	3	4	3
$(^{87}Sr/^{86}Sr)_{269Ma}$	0.703559	0.70338	0.703672	0.703668	0.703652	0.703635	0.70359
Nd($\times10^{-6}$)	3.19	3.1	3.69	3.36	3.79	4.26	6.39
Sm($\times10^{-6}$)	0.75	0.84	0.83	0.88	0.97	1	1.62
$^{143}Nd/^{144}Nd$	0.512805	0.512916	0.512889	0.512903	0.512895	0.512907	0.512907
$2\sigma_m$	3	5	3	3	4	6	2
$(^{143}Nd/^{144}Nd)_{269Ma}$	0.512555	0.512628	0.51265	0.512624	0.512623	0.512657	0.512637
$\varepsilon_{Nd(269Ma)}$	5.14	6.56	6.99	6.49	6.46	7.14	6.75
Th($\times10^{-6}$)			0.56	0.56	0.6	0.54	0.57
U ($\times10^{-6}$)			0.23	0.19	0.216	0.2	0.24
Pb($\times10^{-6}$)			1.72	1.66	2.48	1.75	2.8
$^{208}Pb/^{204}Pb$			37.875	37.884	37.874	37.861	37.78
Std err			0.003	0.003	0.002	0.003	0.003
$^{207}Pb/^{204}Pb$			15.495	15.475	15.468	15.473	15.489
Std err			0.001	0.001	0.001	0.001	0.001
$^{206}Pb/^{204}Pb$			18.554	18.391	18.371	18.348	18.376
Std err			0.002	0.001	0.001	0.001	0.001
$(^{206}Pb/^{204}Pb)_{269Ma}$			18.19	18.08	18.13	18.04	18.15
$(^{207}Pb/^{204}Pb)_{269Ma}$			15.48	15.46	15.46	15.46	15.48
$(^{208}Pb/^{204}Pb)_{269Ma}$			37.59	37.59	37.66	37.59	37.6

注: Rb-Sr、Sm-Nd **同位素计算参数:** $\lambda(Sr)=1.42\times10^{-11}a^{-1}$, $\lambda(Nd)=0.654\times10^{-11}a^{-1}$, $(^{87}Sr/^{86}Sr)_{CHUR}=0.7045$, $(^{143}Nd/^{144}Nd)_{CHUR}=0.512638$; Pb **初始同位素计算参数:** $\lambda_1=1.55125\times10^{-10}a^{-1}$, $\lambda_2=9.8485\times10^{-10}a^{-1}$, $\lambda_3=0.49475\times10^{-10}a^{-1}$, $t=269Ma$

表 3 黄山-镜儿泉成矿带主要含矿岩体成岩年龄及铜镍储量

Table 3 Ages and Ni and Cu reserves of the main Cu-Ni sulfide ore-bearing intrusions of the Huangshan-Jingerquan mineralization belt

岩体名称	所测矿物/岩石	测试方法	年龄(Ma)	镍铜储量($\times10^4$t)	资料来源
黄山西	锆石/闪长岩	SHRIMP U-Pb	269±2	32, 20	Qin *et al.*, 2003; Zhou *et al.*, 2004
	锆石/辉长岩	LA-ICP-MS U-Pb	284.5±2.5		Qin *et al.*, 2003; 顾连兴等, 2006
黄山东	锆石/橄榄苏长岩	SHRIMP U-Pb	274±3	36, 17	Qin *et al.*, 2003; 韩宝福等, 2004
	矿石	Re-Os 等时线	282±20		毛景文等, 2002; Qin *et al.*, 2003
香山	锆石/苏长辉长岩	SHRIMP U-Pb	285±1.2	12, 8	Qin *et al.*, 2003
	硫化物/矿石	Re-Os 等时线	298±1.7		Qin *et al.*, 2003; 李月臣等, 2006
葫芦	矿石	Re-Os 等时线	283±13	8.02, 3.96	陈世平等, 2005
图拉尔根		—	—	10.96, 6	三金柱等, 2007

目前多数学者(Wilson, 1989; Campbell, 1993)认为地幔柱活动的主要特征包括:(1)短时间内大规模的幔源岩浆活动(1~2Ma)(Mahoney and Coffey, 1997),如:近年来越来越精确的年龄数据显示峨眉大火成岩省镁铁-超镁铁侵入体形成于259±1Ma(Zhou *et al.*, 2006, 2008; Zhong and Zhu, 2006; Zhong *et al.*, 2009),玄武质岩浆活动的时限仅1~

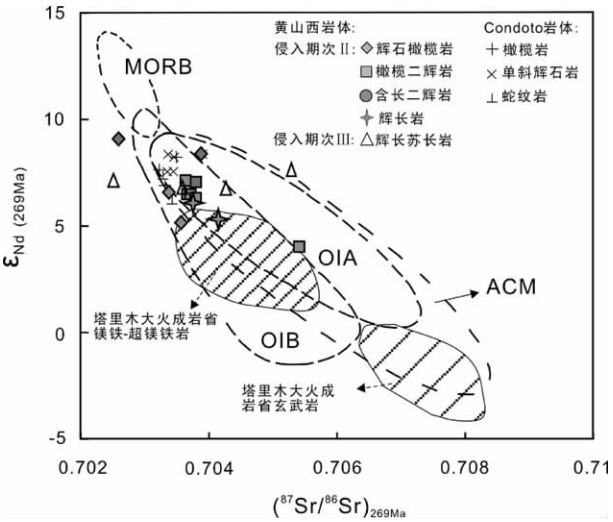

图5 黄山西岩体 $\varepsilon_{Nd(269Ma)}$-$(^{87}Sr/^{86}Sr)_{269Ma}$ 相关图(据 Song and Li, 2009)

黄山西岩体部分数据来自 Zhou *et al.* (2004) **和夏明哲(2009), 塔里木大火成岩省数据来自姜常义等** (2004a, b, c)、Zhang *et al.* (2008) **和** Zhou *et al.* (2009); **洋岛玄武岩**(OIB)、**岛弧**(OIA)、**活动大陆边缘**(ACM) **数据分别来自** Hawkesworth (1982)、Hickey *et al.* (1986) **和** Wilson (1989); Condoto **岩体为阿拉斯加型岩体**(Tistl *et al.*, 1994)

Fig. 5 Diagram of $\varepsilon_{Nd(269Ma)}$ versus $(^{87}Sr/^{86}Sr)_{269Ma}$ of the Huangshanxi intrusive rocks (after Song and Li, 2009)

Some data of Huangshanxi intrusion are cited from Zhou *et al.* (2004) and Xia (2009); the data of Tarim large igneous province are from Jiang *et al.* (2004a, b, c), Zhang *et al.* (2008), Zhou *et al.* (2009); the data of oceanic island basalt (OIB), oceanic island arc (OIA), and active continent margin (ACM) are from Hawkesworth (1982) and Hickey *et al.* (1986), Condoto intrusion is an Alaskan-type complex (Tistl *et al.*, 1994)

2Ma (Ali *et al.*, 2002), **俄罗斯西伯利亚地幔柱的活动时间是** 251.7 ± 0.3Ma, **玄武质岩浆的活动时限为** 1Ma (Kamo *et al.*, 2003); (2) **形成大面积的无沉积夹层的溢流玄武岩和同源镁铁-超镁铁侵入体, 一般属于拉斑玄武岩岩浆系列, 尽管或多或少遭受了地壳混染, 但这些岩石仍具有不少与** OIB (**洋岛玄武岩**) **类似的地球化学特征, 地幔源区是干的, 挥发份含量非常低**; (3) **可能形成大型-超大型岩浆矿床, 如: 俄罗斯** Noril'sk **岩浆** Ni-Cu-PGE **矿床**(Naldrett *et al.*, 1992; Arndt *et al.*, 2003)、**我国峨眉大火成岩省的杨柳坪** Ni-Cu-PGE **矿床**(Song *et al.*, 2003) **和攀枝花钒钛磁铁矿矿床**(宋谢炎等, 2005; Zhou *et al.*, 2005)。

6.1 黄山西岩体与大火成岩省镁铁超镁铁岩体地质特征对比

首先, 黄山-镜儿泉成矿带镁铁-超镁铁岩体的形成年龄在 274 ~ 298Ma **之间**(**表** 3, **除黄山西闪长岩的年龄为** 269Ma (Zhou *et al.*, 2004)), **岩体之间年龄差距超过** 20Ma, **因此, 黄山-镜儿泉成矿带镁铁-超镁铁岩体不具备地幔柱岩浆活动典型特征, 并且其形成时间明显早于塔里木大火成岩省镁铁-超镁铁岩体**(272 ~ 274Ma, **李勇等**, 2007)。

其次, 黄山-镜儿泉成矿带缺少与塔里木地幔柱同时代和相同地球化学特征的溢流拉斑玄武岩。在微量元素蛛网图中, 岩体配分模式与 OIB、**地幔柱有关的力马河岩体和塔里木大火成岩省瓦吉里塔格岩体及巴楚辉绿岩墙明显不同, 力马河岩体、瓦吉里塔格岩体和巴楚辉绿岩墙微量元素都高于黄山西岩体,** Nb、Ta **和** Ti **的亏损程度也远远弱于黄山西岩体, 这说明黄山西岩体岩浆源区不同于大火成岩省镁铁-超镁铁岩体。另外, 塔里木地幔柱玄武岩** $\varepsilon_{Nd}(t)$ **为** −9.27 ~ −1.73(**姜常义等**, 2004c; Zhou *et al.*, 2009), **镁铁-超镁铁岩体的** $\varepsilon_{Nd}(t)$ (0.25 ~ 5.352) (**姜常义等**, 2004a, b; Zhang *et al.*, 2008; Zhou *et al.*, 2009) **明显低于黄山西岩体** $\varepsilon_{Nd}(t)$ (+6.7 ~ +9.3) (Zhou *et al.*, 2004), **所以两个地区的镁铁-超镁铁岩浆可能来自不同的源区。**

姬金生等(1994)、**左国朝等**(2006) **和侯广顺等**(2006) **认为黄山-镜儿泉成矿带石炭纪火山岩是岛弧火山岩或弧后盆地环境形成; 成矿带内二叠纪花岗岩**(250 ~ 310Ma) **和众多的镁铁-超镁铁岩为碰撞后幔源岩浆底侵和内侵作用形成** (Jahn *et al.*, 2000; **王京彬和徐新**, 2006; **顾连兴等**, 2006)。**综上所述, 黄山-镜儿泉铜镍成矿带含矿镁铁-超镁铁岩体的形成与地幔柱无关。**

6.2 黄山西岩体岩浆源区特征

在 MORB **标准化微量元素蛛网图中, 黄山西岩体岩石微量元素配分模式类似于阿拉斯加型** Quetico **岩体, 而与塔里木大火成岩省侵入岩体、峨眉山大火成岩省含铜镍硫化物的力马河岩体和洋岛玄武岩具有明显的区别**(**图** 4)。

Nb、Ta、Ti **负异常是受俯冲事件交代地幔部分熔融岩浆的典型特点之一, 在岛弧系统中, 地幔楔受流体交代作用, 如果在交代过程中角闪石发生分异或者在地幔楔发生部分熔融时金红石及榍石作为残留相, 都会使得产生的岩浆中亏损** Nb、Ta、Ti (**张本仁和傅家谟**, 2005; Ionov and Hofmann, 1995)。**因此, 黄山西岩体** Nb、Ta、Ti **负异常指示岩体的地幔源区可能经历了俯冲事件的交代作用。在** Sr-Nd **同位素图解中, 黄山西岩体投影在岛弧及活动大陆边缘区域内, 与阿拉斯加型镁铁-超镁铁岩体相似, 但不同于洋岛玄武岩和塔里木大火成岩省玄武岩及侵入岩体**(**图** 5), **而且黄山西岩体含有许多的含水矿物**(**如角闪石、黑云母**), **这些特征暗示其原始岩浆来自交代地幔的部分熔融。**

如前所述, 地幔楔受流体交代作用会使得产生的岩浆中亏损 Nb、Ta、Ti, **从而使分配系数相近的不相容元素**(**如** La、Ba、Th、Nb) **发生明显的分异, 因此较高的** La/Nb **和** Ba/Na **比值和较低的** Nb/Th **比值可以作为地幔楔遭受流体交代强度的指标。首先, 在** $\varepsilon_{Nd(269Ma)}$-Ba/Nb、$\varepsilon_{Nd(269Ma)}$-La/Nb **和** $\varepsilon_{Nd(269Ma)}$-

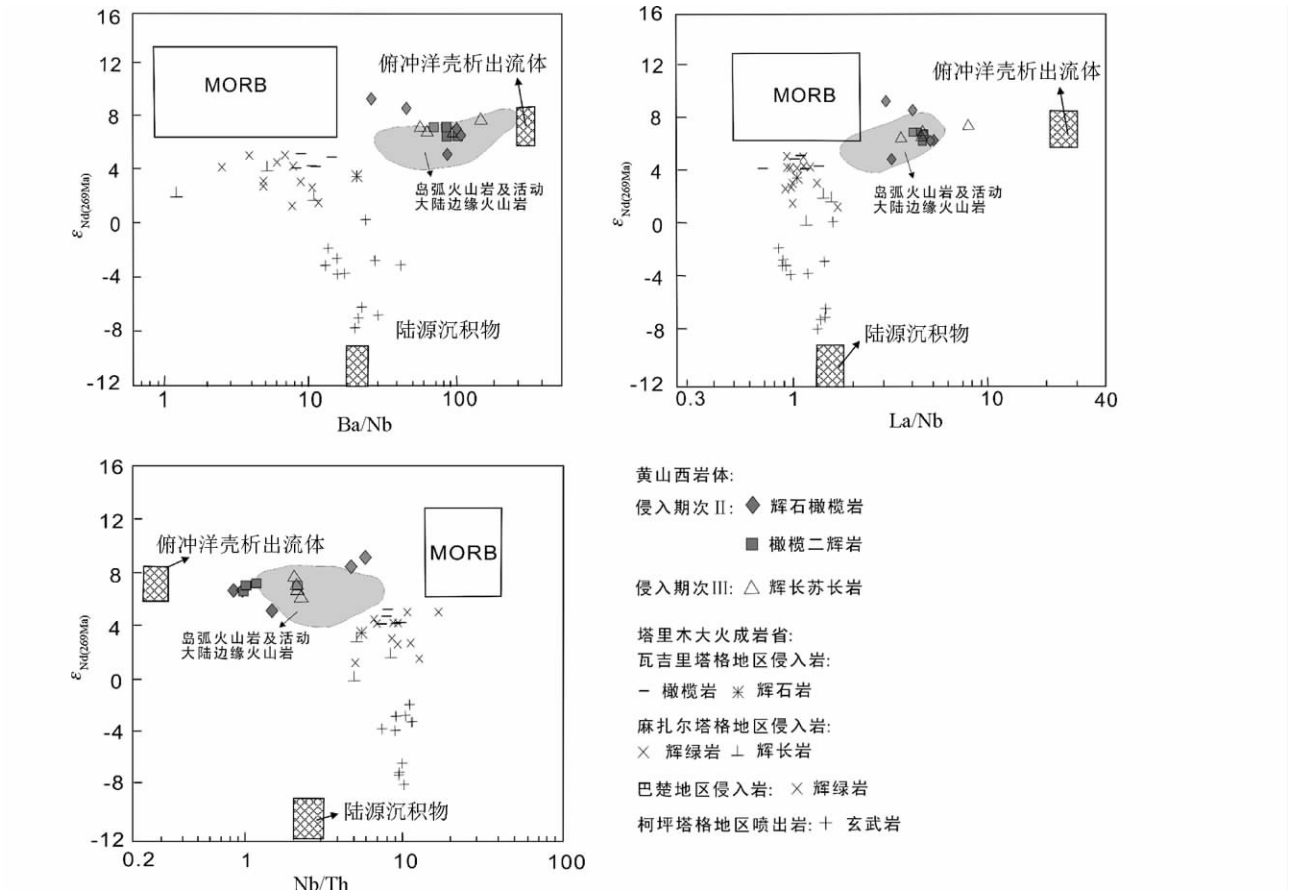

图 6 黄山西岩体 $\varepsilon_{Nd(269Ma)}$-Ba/Nb、$\varepsilon_{Nd(269Ma)}$-La/Nb 和 $\varepsilon_{Nd(269Ma)}$-Nb/Th 图(据 Li, 1994)

黄山西岩体部分数据来自 Zhou *et al.* (2004), **瓦吉里塔格地区(姜常义等, 2004a)、麻扎尔塔格地区(姜常义等, 2004b)、巴楚地区(** Zhou *et al.* (2009) **镁铁-超镁铁岩和柯坪塔格地区玄武岩(姜常义等, 2004c;** Zhou *et al.*, 2009) **为塔里木大火成岩省岩浆岩; 岛弧火山岩数据来自** Elliott *et al.* (1997), **活动大陆边缘火山岩数据来自** Kozlovsky *et al.* (2006)

Fig. 6 Diagrams of $\varepsilon_{Nd(269Ma)}$ versus Ba/Nb, La/Nb and Nb/Th of the Huangshanxi intrusive rocks (after Li, 1994)

Some data of Huangshanxi intrusive rocks are from Zhou *et al.* (2004), the intrusive rocks of Wajilitag (Jiang *et al.* 2004a), Mazhartag (Jiang *et al.*, 2004b), Bachu (Zhou *et al.*, 2009) and basalts of Keping (Jiang *et al.*, 2004c; Zhou *et al.*, 2009) are in the Tarim large igneous province; the data of oceanic island arc and active continental margin are from Elliott *et al.* (1997) and Kozlovsky *et al.* (2006)

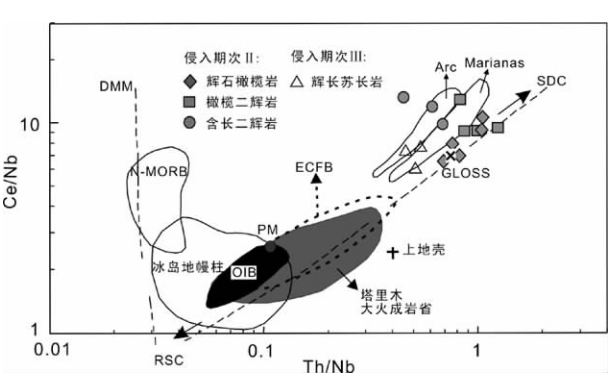

图 7 黄山西岩体 Th/Nb-Ce/Nb 图解(据 Song *et al.*, 2004)

塔里木大火成岩省数据来自姜常义等 (2004a, b, c), Zhang *et al.* (2008) **和** Zhou *et al.* (2009)

Fig. 7 Diagram of Th/Nb versus Ce/Nb of Huangshanxi intrusive rocks (after Song *et al.*, 2004)

Data of Tarim large igneous province from Jiang *et al.* (2004a, b, c), Zhang *et al.* (2008), Zhou *et al.* (2009)

Nb/Th **图中(图 6), 黄山西岩体与岛弧玄武岩投影相似, 与塔里木大火成岩省瓦吉里塔格地区超镁铁岩、麻扎尔塔格地区和巴楚地区辉绿岩墙及柯坪塔格地区玄武岩明显不同, 证明黄山西岩体原始岩浆源于与俯冲洋壳析出流体产生的交代地幔, 而与塔里木地幔柱有关的瓦吉里塔格地区超镁铁岩、麻扎尔塔格地区和巴楚地区辉绿岩墙及柯坪塔格地区玄武岩低的** La/Nb、Ba/Nb **和高的** Nb/Th **表明它们的源区与俯冲洋壳析出流体产生的地幔交代作用无关, 它们在图** 6 **中位于** MORB **和陆源碎屑物之间, 指示它们的原始岩浆与重新进入对流上地幔的陆源沉积物有关(图** 6**)。其次, 在** Th/Nb–Ce/Nb **图解中(图** 7**), 黄山西岩体样品投点在** MORB **与俯冲循环物质之间, 岛弧环境区域, 而与洋岛玄武岩、峨眉山大火成岩省玄武岩和塔里木大火成岩省岩石有明显的差别, 这也说明黄山西岩体岩浆可能来源于俯冲物质析出流体交代的地幔, 而非地幔柱构造形成。此外,** Pb **作为活泼的流体活动性元素在俯冲板片的脱水过程中会进入地幔楔(** Brenan *et*

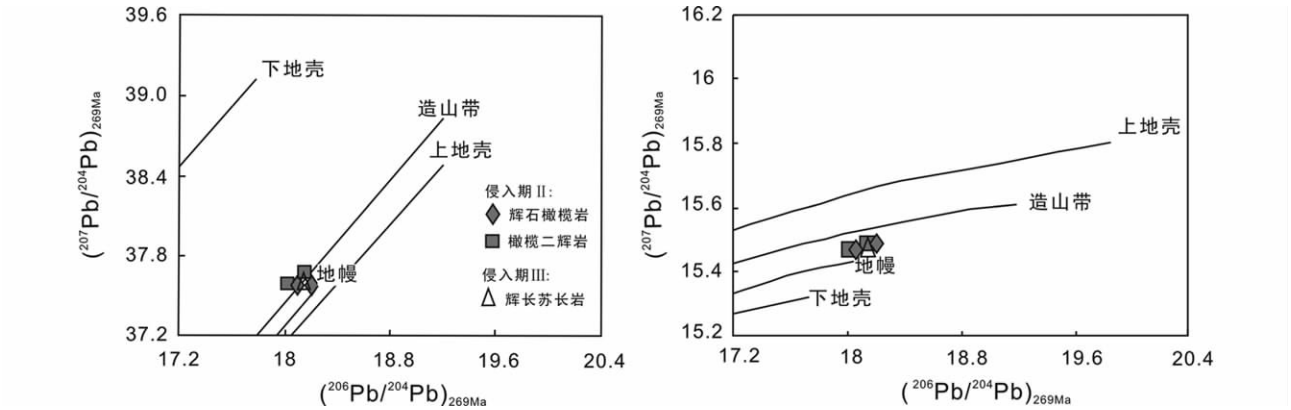

图 8 黄山西岩体 Pb 同位素图解(据 Zartman and Doe, 1981)

Fig. 8 Diagrams of Pb isotopic of the Huangshanxi intrusive rocks (after Zartman and Doe, 1981)

al., 1995)。在地幔部分熔融的情况下,Pb 和 Ce 具有相似的分配系数,但是在流体中,Ce 的分配系数比 Pb 偏大,从而使岛弧玄武岩 Ce/Pb(~3)明显低于洋岛玄武岩(10.7~25)、洋中脊玄武岩(10.7~25)及地球平均值(~10)(Miller *et al.*, 1994; Brenan *et al.*, 1995)。黄山西 Ce/Pb 在 0.88~3.88 之间,平均为 2.49;说明黄山西岩体与岛弧玄武岩相似,源区为受到俯冲洋壳析出流体交代过的地幔。

同时,黄山西岩体的 Pb 同位素比值较低,$^{206}Pb/^{204}Pb_{(269Ma)}$ 比值为 18.04~18.19,$^{207}Pb/^{204}Pb_{(269Ma)}$ 比值为 15.46~15.48,$^{207}Pb/^{204}Pb_{(269Ma)}$ 比值为 37.59~37.66,与太平洋洋中脊玄武岩、蚀变洋壳析出流体平均值接近($^{206}Pb/^{204}Pb$ = 18.35,$^{207}Pb/^{204}Pb$ = 15.48,$^{207}Pb/^{204}Pb$ = 37.8),而且明显低于平均沉积物数值($^{206}Pb/^{204}Pb$ = 18.77,$^{207}Pb/^{204}Pb$ = 15.65,$^{207}Pb/^{204}Pb$ = 38.83)和大陆地壳平均值($^{206}Pb/^{204}Pb$ = 19.22,$^{207}Pb/^{204}Pb$ = 15.78,$^{207}Pb/^{204}Pb$ = 39.58)(Ishizuka *et al.*, 2003; Staudigel *et al.*, 1996)。在 Pb 同位素图解中,黄山西样品数据投点在造山带演化线附近,靠近地幔演化线一侧(图 8),说明岩体原始岩浆在侵位过程中地壳同化混染作用较弱。

上述讨论都说明黄山西岩体的地幔源区为受俯冲事件改造的交代地幔,可能形成于活动大陆边缘,岩浆起源直接与洋壳俯冲有关(Xiao *et al.*, 2008, 2009)。但黄山西岩体的岩相分布与典型的阿拉斯加型同心环状杂岩体有不少区别。大量研究表明,阿拉斯加型岩体一般呈完整或不完整的管状,具有纯橄榄岩核部,向外依次为辉石橄榄岩,橄榄单斜辉石岩,角闪单斜辉石岩和角闪岩;岩石中辉石几乎都是单斜辉石,很少见或者缺失有斜方辉石,磁铁矿在橄榄辉石岩、角闪辉石岩和角闪岩中的含量高,体积分数可以高达 15%~20%(Taylor *et al.*, 1967; Findlay, 1969; Irvine, 1974; Thakurta *et al.*, 2008; Ripley, 2009)。而黄山西岩体不具环状岩相分布,岩体顶部的橄榄岩相是无根的上悬体,为最早的侵入相;其次,辉石橄榄岩、橄榄二辉岩和含长二辉岩的斜方辉石含量可达 30%~40%,而磁铁矿含量小于 5%。

鉴于东天山地区的俯冲碰撞事件结束于晚石炭世,二叠世该地区已进入碰撞后阶段(Zhou *et al.*, 2004; 韩宝福等, 2004; 王京彬等, 2006; 李锦轶等, 2006; 顾连兴等, 2006; Mao *et al.*, 2008),本文认为不能排除黄山西岩体形成于碰撞造山后的伸展阶段可能性。由于软流圈上涌导致被石炭世俯冲事件改造的交代地幔发生部分熔融,在较低的温度下可以形成高镁钙碱性玄武岩浆,黄山西及黄山-镜儿泉铜镍成矿带上其它含矿岩体与这种高镁钙碱性玄武岩浆的侵入有关,其形成过程与喀拉通克含矿岩体的成因类似(Song and Li, 2009)。

7 结论

(1) 黄山西岩体地球化学特征与俯冲有关的岛弧火山岩及阿拉斯加型岩体相似,显示其地幔源区为受俯冲事件改造过的交代地幔。

(2) 黄山西岩体地质与地球化学特征与塔里木大火成岩省镁铁-超镁铁岩体及玄武岩有明显的区别,岩体直接由塔里木地幔柱岩浆活动形成的可能性较小。

(3) 虽然黄山西岩体地球化学特征与俯冲有关的阿拉斯加型岩体相似,但是两者岩石学特征存在差异,指示岩体并非形成于俯冲环境中,岩浆起源可能与造山后软流圈上涌有关。

致谢 本次研究的野外工作得到了新疆地矿局第六地质大队莫新华、马丽华工程师以及其他工程技术人员的大力协助,实验分析得到了中科院地球化学研究所矿床地球化学国家重点实验室胡静老师、黄艳老师和冯彩霞副研究员的帮助,审稿人对本文提出了建设性修改意见,在此谨致谢意。

References

Ali JR, Thompson GM, Song XY and Wang Y. 2002. Emeishan basalts

(SW China) and the 'end-Guangdalupian' crisis: Magnetobiostratigraphic constraints. Journal of the Geological Society, 159: 21 – 29

Arndt NT, Czamanske GK, Walker RJ, Chauvel C and Fedorenko VA. 2003. Geochemistry and origin of the intrusive hosts of the Nori'sk–Talnakh Cu–Ni–PGE sulfide deposits. Economic Geology, 98: 494 – 515

Bai YL. 2000. Geotectonic setting of Huangshan–Jingerquan nickel–copper mineralization system in Hami, Xinjiang. Acta Geologica Gansu, 9(2): 1 – 7 (in Chinese with English abstract)

Bureau of Geology and Mineral Resources of Xinjiang Uygur Autonomous Region (BGMRX). 1993. Region Geology of Xinjiang Autonomous Region. Beijing: Geological Publishing House, 1 – 841 (in Chinese)

Brenan J, Shaw H and Ryerson F. 1995. Experimental evidence for the origin of lead enrichment in convergent-margin magmas. Nature, 378 (2): 54 – 56

Campbell I. 1993. The evolution of the mantle's chemical structure. Lithos, 30(3): 389 – 399

Chen SP, Wang DH, Qu WJ, Chen ZH and Gao XL. 2005. Geological features and ore formation of the Hulu Cu–Ni sulfide deposit, eastern Tianshan, Xinjiang. Xinjiang Geology, 23(3): 230 – 233 (in Chinese with English abstract)

Elliott T, Plank T, Zindler A, White W and Bourdon B. 1997. Element transport from slab to volcanic front at the Mariana arc. Journal of Geophysical Research-Solid Earth, 102(B7): 14991 – 15019

Findlay DC. 1969. Origin of the Tulameen ultramafic–gabbro complex, southern British Columbia. Can. J. Earth Sci., 6(3): 399 – 425

Gu LX, Zhang ZZ, Wu CZ, Wang YX, Tang JH, Wang CS, Xi AH and Zheng YC. 2006. Some problems on granites and vertical growth of the continental crust in the eastern Tianshan Mountains, NW China. Acta Petrologica Sinica, 22(5): 1103 – 1120 (in Chinese with English abstract)

Han BF, Ji JQ, Song B, Chen LH and Li ZH. 2004. Zircon SHRIMP U–Pb age and geology of Kalatongke–Huangshan mafic-ultramafic complex, Xinjiang, China. Chinese Science Bulletin, 49(22): 2324 – 2328 (in Chinese)

Hawkesworth C. 1982. Isotope characteristics of magmas erupted along destructive plate margins. Andesites: Orogenic Andesites and Related Rocks. New York: John Wiley, 549 – 571

Hickey R, Frey F and Gerlach D. 1986. Multiple sources for basaltic arc rocks from the southern volcanic zone of the Andes (34 – 41 S): Trace element and isotopic evidence for contributions from subducted oceanic crust, mantle, and continental crust. Journal of Geophysical Research, 91: 5963 – 5984

Hong D, Zhang J, Wang T, Wang S and Xie X. 2004. Continental crustal growth and the supercontinental cycle: Evidence from the Central Asian Orogenic Belt. Journal of Asian Earth Sciences, 23 (5): 799 – 813

Hou GS, Tang HF and Liu CQ. 2006. Geochemical characteristics of the Late Paleozoic volcanics in Jueluotage tectonic belt, eastern Tianshan and its implications. Acta Petrologica Sinica, 22(5): 1167 – 1177 (in Chinese with English abstract)

Hu SX, Guo JC and Gu LX. 1990. Geology of the Caledonian orogenic belt and its importance to the framework of East Tianshan (E85° ~ E95°). Geoscience of Xinjiang. Beijing: Geological Publishing House, 1: 32 – 45 (in Chinese with English abstract)

Ionov DA and Hofmann AW. 1995. Nb–Ta-rich mantle amphiboles and micas: Implication for subduction-related metasomatic trace element fractionations. Earth Planet. Sci. Lett., 131(3 – 4): 341 – 356

Irvine T and Baragar W. 1971. A guide to the chemical classification of the common volcanic rocks. Canadian Journal of Earth Sciences, 8 (5): 523 – 548

Irvine T. 1974. Petrology of the Duke Island ultramafic complex, southeastern Alaska. Geol. Soc. America Memoir, 138: 1 – 240

Ishizuka O, Taylor R, Milton J and Nesbitt R. 2003. Fluid-mantle interaction in an intra-oceanic arc: Constraints from high-precision Pb isotopes. Earth and Planetary Science Letters, 211(3 – 4): 221 – 236

Jahn BM, Wu FY and Chen B. 2000. Massive granitoid generation in Central Asia: Nd isotope evidence and implication for continental growth in the Phanerozoic. Episodes, 23(2): 82 – 92

Ji JS, Tao HX and Yang XK. 1994. Geochemical characteristics of volcanic rocks within different tectonic settings in the central part of east Tianshan Mountains. Acta Petrologica et Mineralogica, 13(4): 297 – 304 (in Chinese with English abstract)

Jiang CY, Zhang PB, Lu DR and Bai KY. 2004a. Petrogenesis and magma source of the ultramafic rocks at Wajilitag region, western Tarim plate in Xinjiang. Acta Petrologica Sinica, 20(6): 1433 – 1444 (in Chinese with English abstract)

Jiang CY, Jia CZ, Li LC, Zhang PB, Lu DR and Bai KY. 2004b. Source of the Fe-riched-type high-Mg magma in Mazhartag region, Xinjiang. Acta Geologica Sinica, 78(6): 770 – 780 (in Chinese with English abstract)

Jiang CY, Zhang PB, Lu DR, Bai KY, Wang YP, Tang SH, Wang JH, Yang C and 2004c. Petrology, geochemistry and petrogenesis of the Kalpin basalts and their Nd, Sr and Pb isotopic compositions. Geological Review, 50(5): 492 – 500 (in Chinese with English abstract)

Kamo SL, Czamanske GK, Amelin Y, Fedorenko VA, Davis DW and Trofimov VR. 2003. Rapid eruption of Siberian flood-volcanic rocks and evidence for coincidence with the Permian–Triassic boundary and mass extinction at 251Ma. Earth and Planetary Science Letters, 214 (1 – 2): 75 – 91

Kozlovsky A, Yarmolyuk V, Savatenkov V and Kovach V. 2006. Sources of basaltoid magmas in rift settings of an active continental margin: Example from the bimodal association of the Noen and Tost ranges of the Late Paleozoic Gobi–Tien Shan rift zone, southern Mongolia. Petrology, 14(4): 337 – 360

Li JY, Wang KZ, Sun GH, Mo SG, Li WQ, Yang TN and Gao LM. 2006. Paleozoic active margin slices in the southern Turfan–Hami basin: Geological records of subduction of the Paleo-Asian ocean plate in Central Asian regions. Acta Petrologica Sinica, 22(5): 1087 – 1102 (in Chinese with English abstract)

Li SG. 1994. Implications of ε_{Nd}–La/Nb, Ba/Nb, Nb/Th diagrams to mantle heterogeneity-classification of island arc basalts and decomposition of EM Ⅱ component. Chinese Journal of Geochemistry, 14(2): 117 – 127

Li Y, Su W, Kong P, Qian YX, Zhang KY, Zhang ML, Chen Y, Cai XJ and You DH. 2007. Zircon U–Pb ages of the Early Permian magmatic rocks in the Tazhong–Bachu region, Tarim basin by LA–ICP–MS. Acta Petrologica Sinica, 23(5): 1097 – 1107 (in Chinese with English abstract)

Li YC, Zhao GC, Qu WJ, Pan CZ, Mao QG and Du AD. 2006. Re-Os isotopic dataing of the Xiangshan deposit, east Tianshan, NW China. Acta Petrologica Sinica, 22(1): 245 – 251 (in Chinese with English abstract)

Liu DQ. 1983. Plate tectonic and distribution of mineral resources. Northwestern Geology, 4(2): 1 – 12 (in Chinese with English abstract)

Ma RS, Shu LS and Sun JQ. 1997. Tectonic Evolution and Metallogeny of Eastern Tianshan Mountains. Beijing: Geological Publishing House, 1 – 202 (in Chinese with English abstract)

Mahoney JJ and Coffey MJ. 1997. Large igneous province: Continental, oceanic, and planetary flood volcanism. AGU Geophys. Monogy, 100: 1 – 438

Mao JW, Yang JM, Qu WJ, Du AD, Wang ZL and Han CM. 2002. Re–Os dating of Cu–Ni sulfide ores from Huangshandong deposit in Xinjiang and its geodynamic significance. Mineral Deposit, 21(4): 323 – 330 (in Chinese with English abstract)

Mao JW, Pirajno F, Zhang ZH, Chai FM, Yang JM, Wu H, Chen SP, Cheng SL and Zhang CQ. 2006. Late Variscan post-collisional Cu–Ni sulfide deposits in East Tianshan and Altay in China: Principal characteristics and possible relationship with mantle plume. Acta Geologica Sinica, 80(7): 927 – 942 (in Chinese with English abstract)

Mao JW, Pirajno F, Zhang ZH, Chai FM, Wu H, Chen SP, Chen LS, Yang JM and Zhang CQ. 2008. A review of the Cu-Ni sulphide deposits in the Chinese Tianshan and Altay orogens (Xinjiang Autonomous Region, NW China): Principal characteristics and ore-forming processes. Journal of Asian Earth Sciences, 32(2-4): 184-203

Miller D, Goldstein S and Langmuir C. 1994. Cerium/lead and lead isotope ratios in arc magmas and the enrichment of lead in the continents. Nature, 368(6471): 514-520

Naldrett AJ, Lightfoot PC, Fedorenko V, Doherty W and Gorbachev NS. 1992. Geology and geochemistry of intrusions and flood basats of the Noril'sk region, USSR, with implications for the origin of the Ni-Cu ores. Economic geology, 87: 975-1004

Pettigrew NT and Hattori KH. 2006. The Quetico intrusions of Western Superior Province: Neo-Archean examples of Alaskan/Ural-type mafic-ultramafic intrusions. Precambrian Research, 149(1): 21-42

Pirajno F, Mao J, Zhang Z and Chai F. 2008. The association of mafic-ultramafic intrusions and A-type magmatism in the Tian Shan and Altay orogens, NW China: Implications for geodynamic evolution and potential for the discovery of new ore deposits. Journal of Asian Earth Sciences, 32(2-4): 165-183

Qi L, Hu J and Conrad G. 2000. Determination of trace elements in granites by inductively coupled plasma ass spectrometry. Talanta, 51: 507-513

Qin KZ. 2000. The orogeny of Central Asia type and mineralization in North Xinjiang. Post-Doctor Research Report. Beijing: Institute of Geology, Chinese Academy of Sciences. 1-194 (in Chinese with English summary)

Qin KZ, Zhang LC, Xiao WJ, Xu XW, Yan Z and Mao JW. 2003. Overview of major Au, Cu, Ni and Fe deposits and metallogenic evolution of the eastern Tianshan Mountains, Northwestern China. In: Mao JW, Goldfarb R, Seltmann R, Wang DH, Xiao WJ and Hart C (eds.). Tectonic Evolution and Metallogeny of the Chinese Altay and Tianshan. London: IAGOD Guidebook Series, 10: 227-248

Ripley EM. 2009. Magmatic sulfide mineralization in Alaskan-type complexes. In: Li CS and Ripley EM (eds.). New Development in Magmatic Ni-Cu and PGE Deposits. Beijing: Geological Publishing House, 7: 219-228

Rudnick R and Fountain D. 1995. Nature and composition of the continental crust: A lower crustal perspective. Rev. Geophys., 33(3): 267-309

San JZ, Hui WD, Qin KZ, Sun H, Xu XW, Liang GH, Wei JY, Kang F and Xiao QH. 2007. Geological characteristics of Tulargen magmatic Cu-Ni-Co deposit in earstern Xinjiang and its exploration direction. Mineral Deposits, 26(3): 307-316 (in Chinese with English abstract)

Sengör AMC, Natal'inB BA and Burtman VS. 1993. Evolution of the Altaid tectonic collage and Palaeozoic crustal growth in Eurasia. Nature(London), 364(6435): 299-307

Song XY, Zhou MF, Cao ZM, Sun M and Wang Y. 2003. Ni-Cu-(PGE) magmatic sulfide deposits in the Yangliuping area, Permian Emeishan igneous province, SW China. Mineralium Deposita, 38(7): 831-843

Song XY, Zhou MF, Cao ZM and Robinson P. 2004. Late Permian rifting of the South China Craton caused by the Emeishan mantle plume? Journal of the Geological Society, 161(5): 773

Song XY, Zhang CJ, Hu RZ, Zhong H, Zhou MF, Ma RZ and Li YG. 2005. Genetic links of magmatic deposits in the Emeishan large igneous province with dynamics of mantle plume. Journal of Mineralogy and Petrology, 25(4): 35-44 (in Chinese with English abstract)

Song XY and Li XR. 2009. Geochemistry of the Kalatongke Ni-Cu-(PGE) sulfide deposit, NW China: Implications for the formation of magmatic sulfide mineralization in a postcollisional environment. Mineralium Deposita, 44(3): 303-327

Staudigel H, Plank T, White B and Schmincke HU. 1996. Geochemical fluxes during seafloor alteration of the basaltic upper oceanic crust: DSDP sites 417 and 418, In: Bebout GE *et al.* (eds.). Subduction: Top to Bottom. AGU Geophys. Monogr, 96: 19-38

Sun SS and McDonough W. 1989. Chemical and isotopic systematics of oceanic basalts: Implications for mantle composition and processes. In: Saunders AD and Norry MJ (eds.). Magmatism in Oceanic Basins. Spec. Publ. Geol. Soc. Lond., 42: 313-345

Tao Y, Hu RZ and Luo TY. 2007. Geochemistry characteristics and metallogenesis of the Limahe mafic-untramafic intrusion, Sichuan. Acta Petrologica Sinica, 23(11): 2785-2800 (in Chinese with English abstract)

Taylor JH. 1967. The zoned ultramafic complexes of southeastern Alaska. In: Wyllie PJ (ed.). Ultramafic and Related Rocks. New York: John Wiley and Sons Incorporated, 97-121

Thakurta J, Ripley E and Li C. 2008. Geochemical constraints on the origin of sulfide mineralization in the Duke Island Complex, southeastern Alaska. Geochemistry Geophysics Geosystems, 9(7): Q07003

Tistl M Burgath KP, Hohndorf A, Kreuzer H, Munoz R and Salinas R. 1994. Origin and emplacement of tertiary ultramafic complexes in northwest Columbia: Evidence from geochemistry and K-Ar, Sm-Nd and Rb-Sr isotopes. Earth and Planetary Science Letters, 126(1-3): 41-59

Wang JB and Xu X. 2006. Post-collisional tectonic evolution and metallogenesis in northern Xinjiang, China. Acta Geologica Sinica, 80(1): 23-31 (in Chinese with English abstract)

Wang JB, Wang YW and He ZJ. 2006. Ore deposits as a guide to the tectonic evolution in the East Tianshan Mountains, NW China. Geology in China, 33(3): 461-469 (in Chinese with English abstract)

Wang YW, Wang JB, Wang LJ and Fang TH. 2004. REE characteristics of Cu-Ni sulfide deposits in the Hami area, Xinjiang. Acta Petrologica Sinica, 20(4): 935-948 (in Chinese with English abstract)

Wilson M. 1989. Igneous Petrogenesis. London: Unwin Hyman, 1-466

Xia MZ. 2009. The mafic-ultramafic intrusions in the Huangshan region eastern Tianshan, Xinjiang: Petrogenesis and mineralization implication. Ph. D. Dissertation. Xian: Chang'an University, 58-76(in Chinese with English summary)

Xiao WJ, Han CM, Yuan C, Sun M, Lin SF, Chen HL, Li ZL, Li JL and Sun S. 2008. Middle Cambrian to Permian subduction-related accretionary orogenesis of Northern Xinjiang, NW China: Implications for the tectonic evolution of central Asia. Journal of Asian Earth Sciences, 32(2-4): 102-117

Xiao WJ, Windley BF, Huang BC, Han CM, Yuan C, Chen HL, Sun M, Sun S and Li JL. 2009. End-Permian to Mid-Triassic termination of the accretionary processes of the southern Altaids: Implications for the geodynamic evolution, Phanerozoic continental growth, and metallogeny of Central Asia. International Journal of Earth Science, 98: 1189-1217

Xiao XC. 1995. Discussion on the classification of ophiolites by spread rate. Acta Petrologica Sinica, 11(Suppl.): 10-23 (in Chinese with English abstract)

Zartman RE and Doe BR. 1981. Plumbotectonics: The model. Tectonophysics, 75(1-2): 135-162

Zhang BR and Fu JM. 2005. Geochemical Progress. Beijing: Chemical Industry Press, 1-302 (in Chinese)

Zhang C, Li X, Li Z, Ye H and Li C. 2008. A Permian layered intrusive complex in the western Tarim Block, northwestern China: Product of a ca. 275Ma mantle plume? The Journal of Geology, 116(3): 269-287

Zhang GC, Cui JY and Gao DS. 1999. Determinations for Isotopes of Lead, Strontium and Neodymium in Rock Samples. Beijing: Standards Press of China, 1-8 (in Chinese)

Zhong H and Zhu WG. 2006. Geochronology of layered mafic intrusions from the Pan-Xi area in the Emeishan large igneous province, SW China. Mineralium Deposita, 41(6): 599-606

Zhong H, Zhu WG, Hu RZ, Xie LW, He DF, Liu F and Chu ZY.

2009. Zircon U-Pb age and Sr-Nd-Hf isotope geochemistry of the Panzhihua A-type syenitic intrusion in the Emeishan large igneous province, Southwest China and implications for growth of juvenile crust. Lithos, 110(1-4): 109-128

Zhou MF, Lesher CM, Yang ZX, Li JW and Sun M. 2004. Geochemistry and petrogenesis of 270Ma Ni-Cu-(PGE) sulfide-bearing mafic intrusions in the Huangshan District, eastern Xinjiang, Northwest China: Implications for the tectonic evolution of the Central Asian orogenic belt. Chemical Geology, 209(3-4): 233-257

Zhou MF, Robinson PT, Lesher CM, Keays RR, Zhang CJ and Malpas J. 2005. Geochemistry, petrogenesis and metallogenesis of the Panzhihua gabbroic layered intrusion and associated Fe-Ti-V oxide deposits, Sichuan Province, SW China. Journal of Petrology, 46(11): 2253

Zhou MF, Zhao JH, Qi L, Su WC and Hu RZ. 2006. Zircon U-Pb geochronology and elemental and Sr-Nd isotope geochemistry of Permian mafic rocks in the Funing area, SW China. Contributions to Mineralogy and Petrology, 151(1): 1-19

Zhou MF, Arndt N, Malpas J, Wang CY and Kennedy A. 2008. Two magma series and associated ore deposit types in the Permian Emeishan large igneous province, SW China. Lithos, 103: 352-368

Zhou MF, Zhao JH, Jiang CY, Gao JF, Wang W and Yang SH. 2009. OIB-like, heterogeneous mantle sources of Permian basaltic magmatism in the western Tarim Basin, NW China: Implications for a possible Permian large igneous province. Lithos, 113: 583-594

Zhu WB, Ma RS and Wang CY. 1996. Tectonic attribute of Huangshan-Jingerquan complex in eastern Xinjiang, China. Scientia Geologica Sinica, 31(1): 22-32 (in Chinese with English abstract)

Zuo GC, Liang GL, Chen J, Zheng Y, Gao JB, Xing DC and Li SX. 2006. Late Paleozoic tectonic framework and evolution in the Jiabaishan area, Qoltag, earstern Tianshan Mountains, Northwest China. Geological Bulletin of China, 25(1-2): 48-57 (in Chinese with English abstract)

附中文参考文献

白云来. 2000. 新疆哈密黄山-镜儿泉镍铜成矿系统的地质构造背景. 甘肃地质学报, 9(2): 1-7

陈世平, 王登红, 屈文俊, 陈郑辉, 高晓理. 2005. 新疆葫芦铜镍硫化物矿床的地质特征与成矿时代. 新疆地质, 23(3): 230-233

顾连兴, 张遵忠, 吴昌志, 王银喜, 唐俊华, 汪传胜, 郗爱华, 郑远川. 2006. 关于东天山花岗岩与陆壳垂向增生的若干认识. 岩石学报, 22(5): 1103-1120

韩宝福, 季建清, 宋彪, 陈立辉, 李宗怀. 2004. 新疆喀拉通克和黄山东含铜镍矿镁铁-超镁铁杂岩体的 SHRIMP 锆石 U-Pb 年龄及其地质意义. 科学通报, 49(22): 2324-2328

侯广顺, 唐红峰, 刘丛强. 2006. 东天山觉罗塔格构造带晚古生代火山岩地球化学特征及意义. 岩石学报, 22(5): 1167-1177

胡受奚, 郭继春. 顾连兴. 1990 加里东造山带在东天山(E85°~E95°)构造格架中的重要地位及其地质特征. 新疆地质科学. 第一辑. 北京: 地质出版社, 32-45

姬金生, 陶洪祥, 杨兴科. 1994. 东天山中段不同构造环境火山岩地球化学特征. 岩石矿物学杂志, 13(4): 297-304

姜常义, 张蓬勃, 卢登蓉, 白开寅. 2004a. 新疆塔里木板块西部瓦吉里塔格地区二叠纪超镁铁岩的岩石成因与岩浆源区, 岩石学报, 20(6): 1433-1444

姜常义, 贾承造, 李良辰, 张蓬勃, 卢登蓉, 白开寅. 2004b. 新疆麻扎尔塔格地区铁富集型高镁岩浆的源区. 地质学报, 78(6): 770-780

姜常义, 张蓬勃, 卢登蓉, 白开寅, 王瑶培, 唐索寒, 王进辉, 杨淳. 2004c. 柯坪玄武岩的岩石学、地球化学、Nd、Sr、Pb 同位素组成与岩石成因. 地质论评, 50(5): 492-500

李锦轶, 王克卓, 孙桂华, 莫申国, 李文铅, 杨天南, 高立明. 2006. 东天山吐哈盆地南缘古生代活动陆缘残片: 中亚地区古亚洲洋板块俯冲的地质记录. 岩石学报, 22(5): 1087-1102

李勇, 苏文, 孔屏, 钱一雄, 张克银, 张明利, 陈跃, 蔡习尧, 尤东华. 2007. 塔里木盆地塔中-巴楚地区早二叠世岩浆岩的 LA-ICP-MS 锆石 U-Pb 年龄. 岩石学报, 23(5): 1097-1107

李月臣, 赵国春, 屈文俊, 潘成泽, 毛启贵, 杜安道. 2006. 新疆香山铜镍硫化物矿床 Re-Os 同位素测定. 岩石学报, 22(1): 245-251

刘德权. 1983. 新疆板块构造与矿产分布. 西北地质, 4(2): 1-12

马瑞士, 舒良树, 孙家齐. 1997. 东天山构造演化与成矿. 北京: 地质出版社, 1-202

毛景文, 杨建民, 屈文俊, 杜安道, 王志良, 韩春明. 2002. 新疆黄山东铜镍硫化物矿床 Re-Os 同位素测定及其地球动力学意义. 矿床地质, 21(4): 323-330

毛景文, Pirajno F, 张作衡, 柴凤梅, 杨建民, 吴华, 陈世平, 程松林, 张长青. 2006. 天山-阿尔泰东部地区海西晚期后碰撞铜镍硫化物矿床: 主要特点及可能与地幔柱的关系. 地质学报, 80(7): 925-942

秦克章. 2000. 新疆北部中亚型造山与成矿作用. 博士后研究工作报告. 北京: 中国科学院地质与地球物理研究所, 1-194

三金柱, 惠卫东, 秦克章, 孙赫, 徐兴旺, 梁光河, 魏俊瑛, 康峰, 肖庆华. 2007. 新疆哈密图拉尔根全岩矿化岩浆铜-镍-钴矿床地质特征及找矿方向. 矿床地质, 26(3): 307-316

宋谢炎, 张成江, 胡瑞忠, 钟宏, 周美夫, 马润则, 李佑国. 2005. 峨眉火成岩省岩浆矿床成矿作用与地幔柱动力学过程的耦合关系. 矿物岩石 25(4): 35-44

陶琰, 胡瑞忠, 漆亮, 罗泰义. 2007. 四川力马河镁铁-超镁铁质岩体的地球化学特征及成岩成矿分析. 岩石学报, 23(11): 2785-2800

王京彬, 徐新. 2006. 新疆北部后碰撞构造演化与成矿. 地质学报, 80(1): 23-31

王京彬, 王玉往, 何志军. 2006. 东天山大地构造演化的成矿示踪. 中国地质, 33(3): 461-469

王玉往, 王京彬, 王莉娟, 方同辉. 2004. 新疆哈密黄山地区铜镍硫化物矿床的稀土元素特征及意义. 岩石学报, 20(4): 935-948

夏明哲. 2009. 新疆东天山黄山岩带镁铁-超镁铁质岩石成因及成矿作用. 博士学位论文. 西安: 长安大学, 58-76

肖序常. 1995. 从扩张速率试论蛇绿岩的类型划分. 岩石学报, 11(增刊): 10-23

新疆维吾尔自治区地质矿产局. 1993. 新疆地质志. 北京: 地质出版社

张本仁, 傅家谟. 2005. 地球化学进展. 北京: 化学工业出版社, 1-302

张桂存, 崔建勇, 高鼎顺. 1999. 岩石中铅、锶、钕同位素测定方法. 北京: 中国标准出版社, 1-8

朱文斌, 马瑞士, 王赐银. 1996. 论新疆东部黄山-镜儿泉杂岩带的构造属性. 地质科学, 31(1): 22-32

左国朝, 梁广林, 陈俊, 郑勇, 高俊宝, 邢德超, 李绍雄. 2006. 东天山觉罗塔格地区夹白山一带晚古生代构造格局及演化. 地质通报, 25(1-2): 48-57